Biochemical and Biophysical Research Communications 450 (2014) 67–72

Contents lists available at ScienceDirect

Biochemical and Biophysical Research Communications

journal homepage: www.elsevier.com/locate/ybbrc

Structure determination of archaea-specific ribosomal protein L46a reveals a novel protein fold

Yingang Feng [a,*], Xiaxia Song [b], Jinzhong Lin [c,1], Jinsong Xuan [b], Qiu Cui [a], Jinfeng Wang [c]

[a] Shandong Provincial Key Laboratory of Energy Genetics, Qingdao Institute of Bioenergy and Bioprocess Technology, Chinese Academy of Sciences, Qingdao, Shandong 266101, China
[b] Department of Biological Science and Engineering, School of Chemical and Biological Engineering, University of Science and Technology Beijing, Beijing 100083, China
[c] National Laboratory of Biomacromolecules, Institute of Biophysics, Chinese Academy of Sciences, Beijing 100101, China

ARTICLE INFO

Article history:
Received 9 May 2014
Available online 26 May 2014

Keywords:
Ribosomal protein
Protein structure
Archaea
NMR
Protein fold

ABSTRACT

Three archaea-specific ribosomal proteins recently identified show no sequence homology with other known proteins. Here we determined the structure of L46a, the most conserved one among the three proteins, from *Sulfolobus solfataricus* P2 using NMR spectroscopy. The structure presents a twisted β-sheet formed by the N-terminal part and two helices at the C-terminus. The L46a structure has a positively charged surface which is conserved in the L46a protein family and is the potential rRNA-binding site. Searching homologous structures in Protein Data Bank revealed that the structure of L46a represents a novel protein fold. The backbone dynamics identified by NMR relaxation experiments reveal significant flexibility at the rRNA binding surface. The potential position of L46a on the ribosome was proposed by fitting the structure into a previous electron microscopy map of the ribosomal 50S subunit, which indicated that L46a contacts to domain I of 23S rRNA near a multifunctional ribosomal protein L7ae.

1. Introduction

The ribosome, composed by several rRNAs and dozens of ribosomal proteins, is an important cellular machine responsible for the translation of mRNA into proteins [1,2]. During protein synthesis, other protein factors bind to the ribosome to regulate its function [3]. Ribosomal proteins are largely conserved among three domains of life, while a number of ribosomal proteins are specific to one domain, genus, or species [4]. Analysis of ribosomal proteins in three domains of life revealed that Archaea has a reductive evolution process different from that of Bacteria and Eukarya [5]. This reductive evolution of ribosomal proteins in Archaea indicates a progressive elimination of ribosomal protein genes in the course of archaeal evolution, which implies that the last common ancestor of Archaea possessed a more complex ribosome than any of the existent archaeon species [4,5].

Several novel archaea-specific ribosomal proteins, including L45a, L46a, and L47a that exist only in Crenarchaeota, were recently discovered using proteomic methods [6]. The three archaea-specific ribosomal proteins show no sequence homology with other known proteins, so the structure and function of these proteins are unclear. In the genome, their genes are not associated with the general genomic context of the ribosome, but were found together with components of the transcriptional machinery [6]. For example, the gene of L46a is downstream of *tflD*, encoding the TATA binding protein of the transcription factor TFIID. Similar situations have been observed in other archaeal nonuniversal ribosomal proteins, which suggested that there is expanded linkage between transcription and translation in Archaea [7]. Among the three proteins, L46a is the most conserved one, which is conserved in Thermoprotei genera (Fig. 1). Sequence analysis indicated that L46a is a basic protein with a p$I \sim 10$, suggesting that L46a may directly bind to rRNA in the ribosome. In this study, we determined the solution structure of SsoL46a, an L46a protein from the hyperthermophilic archaeon *Sulfolobus solfataricus* P2, by NMR spectroscopy. The structure represents a novel structural fold with a potential rRNA binding surface. The potential position of L46a on the ribosome was identified by fitting the structure into a previous electron microscopy map of the ribosome.

2. Materials and methods

2.1. Protein expression and purification

The gene of L46a from *S. solfataricus* P2 (Ssol_806108-805899 in The Sulfolobus Database [8], http://www.sulfolobus.org) was

* Corresponding author. Fax: +86 532 80662707.
E-mail address: fengyg@qibebt.ac.cn (Y. Feng).
[1] Current address: Department of Molecular Biophysics and Biochemistry, Yale University, New Haven, CT 06520-8114, USA.

http://dx.doi.org/10.1016/j.bbrc.2014.05.077
0006-291X/

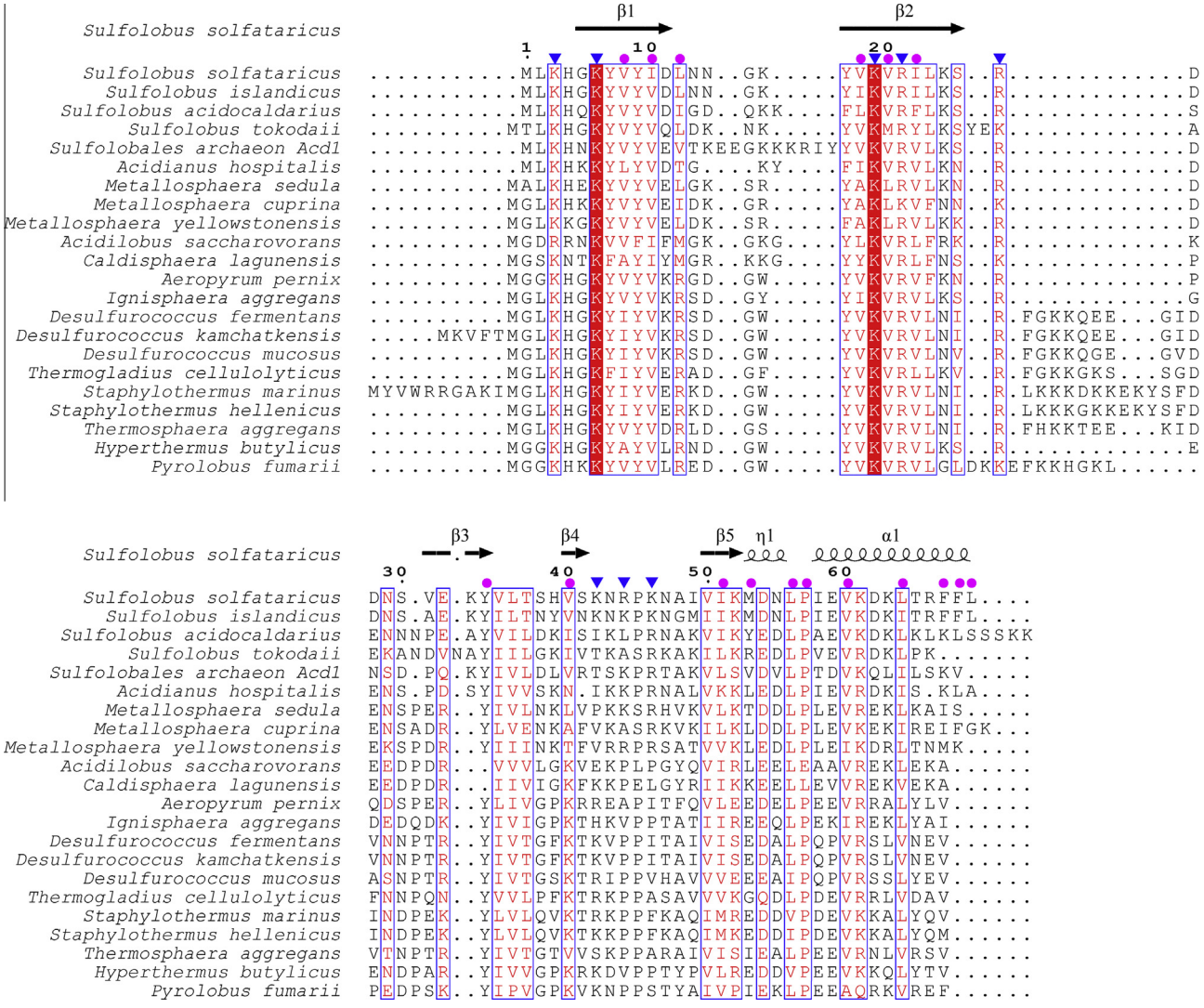

Fig. 1. Sequence alignment of the L46a protein family. Identical residues in the alignments are shown with white characters in red box, while similar residues are shown with red characters. The identical and similar residues are shown in blue frame. The secondary structures of SsoL46a are shown above the sequences. The residues of the hydrophobic core of SsoL46a are indicated by magenta filled circles. The positively charged residues on the potential rRNA-binding surface are indicated by blue triangles. (For interpretation of the references to color in this figure legend, the reader is referred to the web version of this article.)

amplified from the genomic DNA by PCR using two primers 5′-GGCCATATGCTCAAACATGGCAAGTAC-3′ and 5′-GCGCTCGAGTAAAAAGAATCTAGTTAATTTATC-3′. The gene was cloned into the expression vector pET30a between NdeI and XhoI restriction sites, forming a vector pET30a-SsoL46a. The protein product of this construct contains an additional C-terminal His-tag (LEHHHHHH) to facilitate the following protein purification.

The vector pET30a-SsoL46a was transformed into *Escherichia coli* Rosetta(DE3)pLysS. The cells were cultured in M9 minimal medium at 37 °C. When the cell density reached an OD_{600} of about 0.8, the protein expression was induced with 0.4 mM isopropyl-1-thio-β-D-galactopyranoside for 3.5 h at 37 °C. The cells were harvested by centrifugation at 4000*g*, 4 °C for 30 min. The harvested cell pellet was re-suspended in buffer containing 50 mM Tris–HCl, pH 8.0, 1 mM dithiothreitol, 1 mM phenylmethanesulfonyl fluoride, and then frozen at −20 °C overnight. The re-suspended cell pellet was thawed and lysed by sonication. After centrifugation at 15,000*g*, the supernatant of the lysate was treated twice by 70% ammonium sulfate precipitations. The first precipitates were dissolved into 50 mM Tris–HCl, pH 8.0, and the second precipitates were dissolved into 50 mM Tris–HCl, pH 8.0, 1.0 M NaCl. Thereafter, the target protein was purified via a Ni^{2+} Chelating Sepharose Fast Flow (GE Healthcare) column and eluted with 300 mM imidazole. The eluate containing the recombinant SsoL46a was collected and concentrated to 2 mL using Amicon Ultra-15 centrifugal filter units (3.0 kDa cutoff) (Millipore). Then, the protein was further purified using a Superdex 75 (GE Healthcare) gel filtration column pre-equilibrated in 50 mM potassium phosphate buffer (pH 6.8), 1.0 M NaCl, 1.0 mM EDTA. Fractions containing the recombinant SsoL46a with an absorption ratio at 280 nm and 260 nm (A_{280}:A_{260}) greater than 1.2 were collected and dialyzed against 50 mM potassium phosphate buffer (pH 6.0), 50 mM KCl. The protein was finally concentrated to ~1.0 mM using Amicon Ultra-15 centrifugal filter units (3.0 kDa cutoff) (Millipore). Protein concentration was determined by the UV absorption at 280 nm using a theoretical molar extinction coefficient 5120 M^{-1} cm^{-1}.

2.2. NMR spectroscopy

Uniformly ^{15}N- and $^{15}N/^{13}C$-labeled proteins were obtained by growing cells in M9 minimal media containing $^{15}NH_4Cl$ and [^{13}C]-glucose as the sole nitrogen and carbon sources, respectively.

NMR samples consisted of 0.5–1.0 mM recombinant SsoL46a proteins in 90% H_2O/10% D_2O containing 50 mM potassium phosphate buffer (pH 6.0), 50 mM KCl, 2.0 mM EDTA, 0.02%(w/v) sodium 2,2-dimethylsilapentane-5-sulfonate (DSS).

All NMR experiments were performed at 298 K on a Bruker DMX 600 spectrometer equipped with a z-gradient triple-resonance cryoprobe. Backbone and side-chain resonance assignments were derived from two- and three-dimensional spectra including $^{1}H–^{15}N$ HSQC, $^{1}H–^{13}C$ HSQC, HNCACB, CBCA(CO)NH, HNCO, HN(CA)CO, HBHA(CBCA)(CO)NH, HBHA(CBCA)NH, (H)CCH-TOCSY, and $^{1}H–^{15}N$ TOCSY-HSQC. NOE distance constraints were derived from three-dimensional $^{1}H–^{15}N$ NOESY-HSQC spectrum and two three-dimensional $^{1}H–^{13}C$ NOESY-HSQC spectra for aliphatic and aromatic regions. The mixing times for $^{1}H–^{1}H$ TOCSY, $^{13}C–^{13}C$ TOCSY and $^{1}H–^{1}H$ NOESY experiments were 60, 12, and 200 ms, respectively. All NMR spectra were processed using the software Felix (Accelrys Inc.) and analyzed using NMRViewJ [9]. Proton chemical shifts were referenced to the internal DSS, and ^{15}N and ^{13}C chemical shifts were referenced indirectly [10].

2.3. Structural calculation

Initial structures of SsoL46a were generated using CANDID module of CYANA version 2.1 [11]. The structures were refined using CNS version 1.2.1 [12] with NOE-derived distance restraints obtained by SANE [13], backbone dihedral angle restraints obtained using TALOS+[14], and hydrogen-bond restraints according to the initial structures and the regular secondary structure patterns. The structures were further refined in explicit water using CNS and RECOORDScript [15]. A family of 100 structures was generated by CNS, and 50 structures with the lowest energies were subjected to the refinement in explicit water, from which a final set of 20 structures with the lowest energies was selected for the final analysis. The quality of the determined structures was analyzed using MOLMOL [16] and PROCHECK-NMR [17]. MOLMOL and PyMol (DeLano Scientific LLC. http://www.pymol.org) were used for the visualization of the structures. Structural similarity was analyzed using Dali [18], VAST [19], and SSM server [20]. UCSF Chimera version 1.8.1 [21] was used to fit the structure into the electron microscopy map of *Sulfolobus acidocaldarius* 50S ribosomal subunit (EMDataBank 1797, 27 Å resolution).

2.4. Backbone dynamics

Backbone ^{15}N T_1, T_2, and $^{1}H–^{15}N$ steady-state heteronuclear NOE relaxation parameters were measured using standard experiments [22]. The T_1 relaxation delays were set as 20, 40, 80, 120, 160, 250, 400, 650, 1000, 1400, and 1800 ms. The T_2 relaxation delays were set as 16.96, 33.92, 50.88, 67.84, 84.80, 101.76, 118.72, 135.68, 152.64, 169.60, 203.52, 237.44, and 271.36 ms. In $^{1}H–^{15}N$ heteronuclear NOE measurement, a delay of 3 s was followed by a ^{1}H saturation of 3 s, whereas the saturation period was replaced by a delay of 3 s in the control experiment. The two experiments were run in an interleaved manner.

The ^{15}N relaxation rate constants R_1 and R_2 for each residue were determined by nonlinear least squares fitting of the intensities of the cross-peaks in the corresponding 2D NMR spectra to a two-parameter mono-exponential equation: $I(t) = I_0 e^{-R_{1,2}t}$, where I_0 is the peak intensity at $t = 0$ and $I(t)$ is the peak intensity after a time delay t. The $^{1}H–^{15}N$ heteronuclear NOE values were calculated from the ratios of peak intensities measured from the spectra acquired with and without proton saturation. The errors of peak intensities were estimated from spectrum background noise and propagated into the errors of $^{1}H–^{15}N$ heteronuclear NOE values. Monte-Carlo simulations were used to estimate the errors of R_1 and R_2. Model-free analysis of the backbone relaxation data was performed using Modelfree 4.1 [23] and FAST-Modelfree [24].

2.5. Accession numbers

The chemical shifts of SsoL46a were deposited in the BioMagResBank database under the accession number 19860. The atomic coordinates for SsoL46a and all restraints were deposited in the Protein Data Bank database with the accession code 2MMP.

3. Results and discussion

3.1. Chemical shift assignments

Near complete assignments for backbone and side chain ^{1}H, ^{15}N and ^{13}C atoms of SsoL46a were obtained from three-dimensional triple resonance spectra, except for all atoms of residue Met1, H_N and H_γ of Leu2, $H_{\varepsilon1}$ of His4 and His39, and $H_{\delta2}$ and $H_{\varepsilon1}$ of histidine residues 72–77 in the His-tag. The $^{1}H–^{15}N$ HSQC spectrum shows a good dispersion of peaks that were all assigned (Fig. S1). Peaks of four His-tag residues (His73–76) are very weak in the HSQC spectrum, but these peaks were unambiguously assigned because of their strong signals in triple resonance spectra. Peaks of Glu32, Lys33, and Tyr34 are relatively broadened and weak, suggesting that these residues undergo an intermediate conformational/chemical exchange process.

3.2. Structure description

The structure determination of SsoL46a was based on NOE-derived distance, backbone dihedral angle, and hydrogen bond restraints (Table 1). The structure of SsoL46a contains 5 β-strands (β1–β5: residues 5–11, 17–25, 31–34, 40–41, 50–52) and two heli-

Table 1
The experimental restraints and structural statistics for the 20 lowest energy structures of SsoL6a.

Distance restraints	
Intra-residue	688
Sequential	396
Medium	155
Long-range	309
Ambiguous	715
Total	2263
Hydrogen bond restraints	50
Dihedral angle restraints	
φ	58
ψ	58
Total	116
Violations	
Max. NOE violation (Å)	0.171
Max. torsion angle violation (°)	4.63
PROCHECK statistics (%)[a]	
Most favored regions	80.9
Additional allowed regions	16.2
Generously allowed regions	2.7
Disallowed regions	0.2
RMSD from mean structure (Å)	
Backbone heavy atoms	
All residue[a]	1.21 ± 0.36
Regular secondary structure[b]	0.35 ± 0.06
All heavy atoms	
All residue[a]	1.67 ± 0.30
Regular secondary structure[b]	0.82 ± 0.06

[a] The C-terminal 8 residue His-tag (LEHHHHHH) is excluded.
[b] Regular secondary structure regions include residues 5–11, 17–23, 33–34, 40–41, 50–52, 53–55 and 58–67.

ces: one 3_{10} helix (η1: residues 53–55) and one α-helix (α1: residues 58–67) (Fig. 2a and b). The β-strands are antiparallel except that β1–β5 is in parallel, which form a twisted β-sheet structure. β4 is an extension of β3 in anti-parallel to β2. The α-helix is packed on the loops connecting β1 and β2 and connecting β3 and β4. The N-terminal residues 1–4 and the loop $L_{\beta2\beta3}$ (residues 26–30) are poorly defined, suggesting that they are flexible. The C-terminus of β2, the N-terminus of β3, and the loop $L_{\beta4\beta5}$ (residues 42–49) are also not well defined probably because of partial flexibility. The major hydrophobic core of SsoL46a is formed by hydrophobic residues on the β-sheet and helices (Fig. 2c). These residues are largely conserved in the L46a family (Fig. 1), which indicates a conserved structure in the L46a family. The hydrophobic residues at the top of the hydrophobic core are less conserved, suggesting structural variation in this region of the L46a family.

SsoL46a has a high p*I* (~10) and a great number of positively charged residues on the surface, which is typical for a nucleic acid-binding protein. One side of the electrostatic surface of SsoL46a is significantly positively charged, while the other side has both positively and negatively charged surfaces (Fig 2d). It is conceivable that the positively charged side, which includes residues Lys3, Lys6, Lys19, Arg21, Arg26, Lys42, Arg44, and Lys46, forms the rRNA-binding surface. The first five residues are conserved in the L46a protein family (Fig. 1), underlining their key roles in the binding of L46a to the ribosome. Residues Lys42, Arg44, and Lys46 in the loop β4–β5 are less conserved at the sequence level. However, positively charged residues in the same loop is a conserved feature in the L46a family (Fig. 1), suggesting that this loop constitutes an auxiliary part of the binding surface. L46a proteins in several species (lower sequences in Fig. 1) contain a lysine-rich stretch between β2 and β3, which may also extend the rRNA-binding surface.

3.3. Structural comparison – a novel fold

Because there is no sequence similarity found between SsoL46a and other proteins of known structure, we tried to search any structural homologue in the Protein Data Bank using Dali, VAST and SSM servers. The Dali search identified a number of proteins with relatively low *Z*-score (2.0–2.5) and the similarities mainly reside in the four β-strands of similar topology in the structures. However, the strands in these proteins are part of larger β-sheets, indicating their folds are different from SsoL46a. Search using the VAST server returned similar results. Search using the SSM server identified several proteins with size similar to SsoL46a (Fig. 3). These proteins include a chromo shadow domain protein HP1a (PDB 3P7J; *Q*-score 0.14) [25], a protein NE1242 of unknown function (PDB 2JV8; *Q*-score 0.13), and two chromo domain proteins (PDB 2K28 and 3MTS; *Q*-score 0.11) [26]. All these proteins show a large RMSD from the structural alignment, indicating low similarity between SsoL46a and these proteins. Chromo shadow domain and chromo domain have similar topology, and the three proteins containing chromo shadow domain or chromo domain identified by the SSM search show 4.0–5.0 Å RMSDs in the structure alignment with SsoL46a. The protein NE1242 shows the smallest RMSD (3.17 Å) in the structure alignment with SsoL46a. Although these proteins are identified by the SSM search, careful comparison of their topology indicated that they are different from SsoL46a. The β-sheet in chromo shadow or chromo domain contains only three strands, and more importantly, the orientation of these strands are completely different from the strands in SsoL46a (Fig. 3b). The β-sheet of NE1242 contains four strands among which the first three strands are similar to those in the sheet of ssoL46a, but β4 in NE1242 is in anti-parallel to β3, while SsoL46a has a β4 in anti-parallel to β2 as an extension of β3 and an

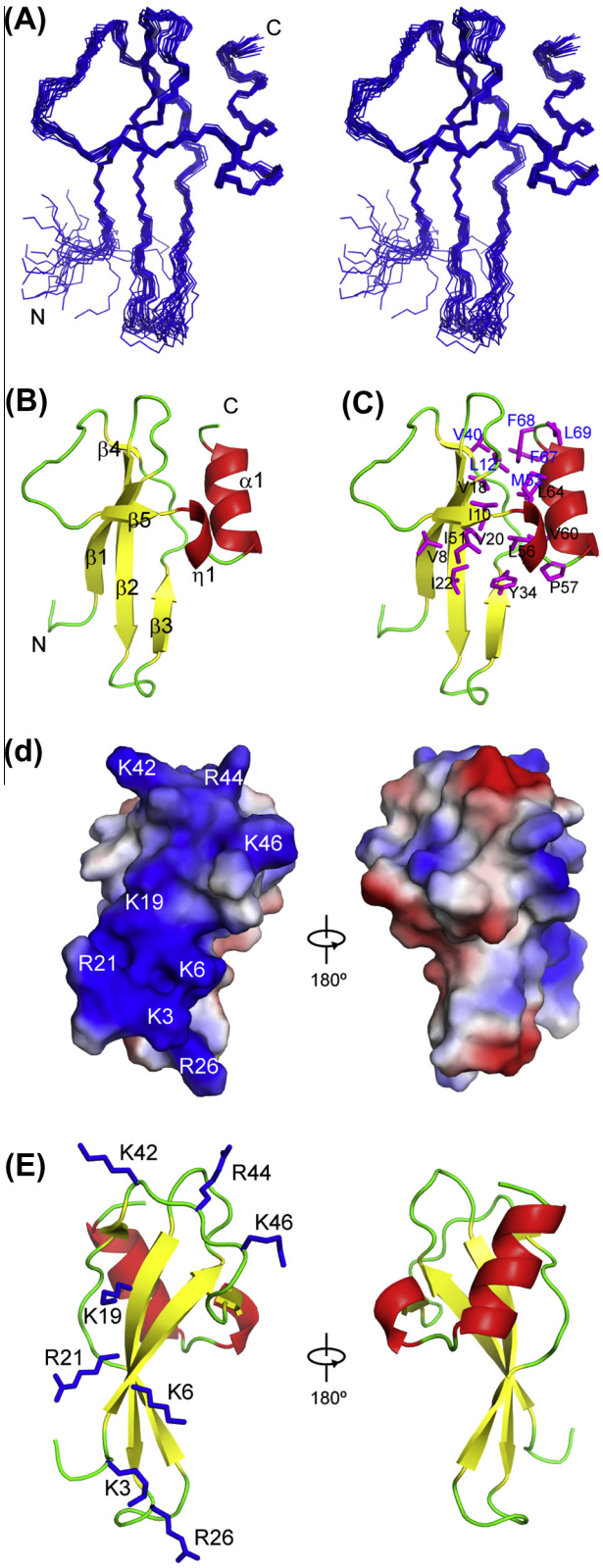

Fig. 2. The structure of SsoL46a. (A) A stereo view of the backbone ensemble of 20 SsoL46a structures determined by NMR. (B) A ribbon representation of the SsoL46a structure. The secondary structures are labeled. (C) The hydrophobic core of SsoL46a. The side chains of residues involved in the hydrophobic core are shown as sticks and labeled with one-letter residue name and sequence number. (D) The electrostatic surface of SsoL46a. Positively charged residues for potential rRNA binding are labeled. (E) A ribbon representation of SsoL46a with the same orientation as in (D).

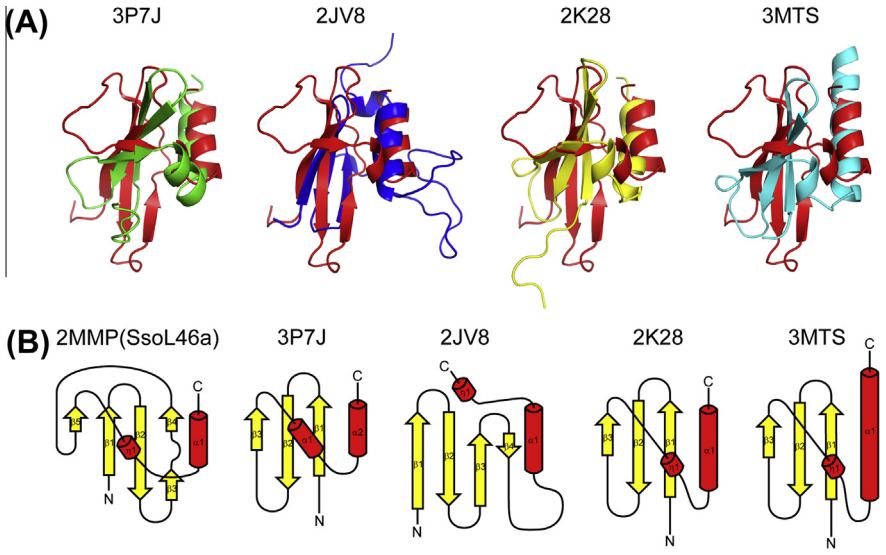

Fig. 3. Structural comparison of SsoL46a and proteins identified by SSM server. (A) Ribbon representation of structures. SsoL46a are shown in red; other proteins were shown in different colors and their PDB numbers are shown on top of the structures. (B) Topology diagrams for comparison of the structure folds. β-strands are shown by yellow arrows, and the helices are shown by red cylinders. (For interpretation of the references to color in this figure legend, the reader is referred to the web version of this article.)

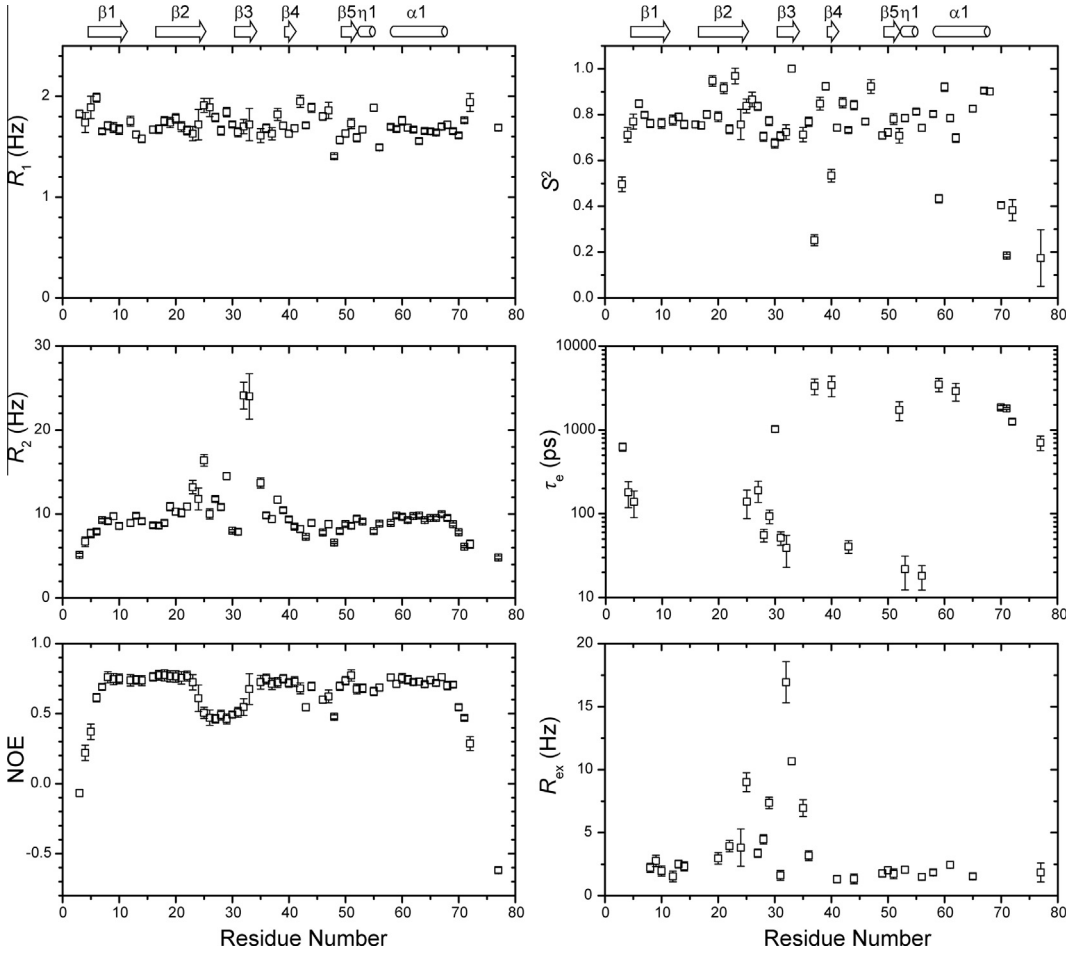

Fig. 4. Backbone relaxation data (R_1, R_2, and ^1H–^{15}N heteronuclear NOE) and model-free dynamics parameters (S^2, τ_e, and R_{ex}) of SsoL46a. The secondary structure elements are marked at the top of the figure.

additional β5 in parallel to β1 after a long loop. SsoL46a has a 3_{10} helix before the C-terminal α-helix, while NE1242 has a 3_{10} helix after the C-terminal α-helix. NE1242 contains a long loop (24 residues) between the sheet and helices. Therefore, the structural topologies of these proteins identified by the SSM search are different from that of SsoL46a. Furthermore, the structural features

related to the functions of these proteins are not conserved. SsoL46a is a ribosomal protein that contains a large positively charged surface to bind rRNA, while the proteins identified by the SSM search do not have this kind of surface. On the other hand, the residues in chromo shadow domain for dimerization and peptide binding, as well as the residues in chromo domain for methylated histone tail binding, are not conserved in SsoL46a. Therefore, these proteins identified by the SSM search are neither structural nor functional homologues to SsoL46a. The structure of SsoL46a represents a novel protein fold.

3.4. Backbone dynamics

The backbone dynamics of SsoL46a were studied by the $^{1}H–^{15}N$ relaxation experiments (Fig. 4). The R_1, R_2 and NOE were estimated and subjected to model-free analysis by the program Modelfree. The overall rotational correlation time τ_m fitted by Modelfree was 4.451 ns, indicating that SsoL46a is a monomer in solution. The dynamics represented by the relaxation data of SsoL46a was in agreement with the structural feature. The N-terminal five residues and C-terminal His-tag (LEHHHHHH) presented small NOE, R_2 and S^2 values, as well as large τ_e values, which indicated that these regions are completely flexible. The loop β2–β3, the C-terminus of β2, and the N-terminus of β3 showed small NOE values but large R_2 values, and in model-free analysis these regions presented significant τ_e and large R_{ex} values, which indicated that these regions are flexible due to internal motions and conformational exchanges. Although the loop β4–β5 showed some flexibility in SsoL46a structure, it only showed slightly smaller NOE values than those in rigid regions, and model-free analysis showed only very small τ_e or R_{ex} in this loop, which indicated that the loop β4–β5 is more restrained than other flexible regions. The regions with significant flexibility are located at the putative rRNA-binding surface, and the flexibility may be beneficial to the binding to rRNA.

3.5. Position of L46a on the ribosome

Previous study by electron microscopy has identified three potential positions (S1–S3) for the three newly discovered ribosomal proteins L45a, L46a, and L47a [6]. The additional density of S1 is the largest, while that of S3 is the smallest. The additional density of S2 is flatter than those of S1 and S3. Among the three ribosomal proteins, L46a is the smallest one, and its large positively charged surface suggested that it binds rRNA directly. When the structure of SsoL46a was docked into the three positions, we found that SsoL46a could be well fitted into the additional density at the S3 position (Fig. S2), while S1 and S2 are too large for the structure of SsoL46a. We propose that SsoL46a contacts domain I of 23S rRNA with the positively charged surface facing the two grooves of rRNA. In the model, SsoL46a does not contact any other ribosomal protein. The nearest ribosomal protein is L7ae, which is a multifunctional protein involved in small nucleolar ribonucleoprotein complexes besides ribosome [27]. Because no information about the stoichiometry of L46a:50S has been reported and the resolution of the EM map is quite low, further experiments in the future are needed to validate our model about the position of L46a on the ribosome, but the unique structure nature of L46a is already clear.

Acknowledgments

This work is supported by the National High-tech R&D Program from Ministry of Science and Technology of China (863 program, grant no. 2012AA02A707) and the National Natural Science Foundation of China (grant nos. 31170701 and 31300635).

Appendix A. Supplementary data

Supplementary data associated with this article can be found, in the online version, at http://dx.doi.org/10.1016/j.bbrc.2014.05.077.

References

[1] V. Ramakrishnan, Ribosome structure and the mechanism of translation, Cell 108 (2002) 557–572.
[2] D.N. Wilson, J.H. Doudna Cate, The structure and function of the eukaryotic ribosome, Cold Spring Harb. Perspect. Biol. 4 (2012) a011536.
[3] S. Xue, M. Barna, Specialized ribosomes: a new frontier in gene regulation and organismal biology, Nat. Rev. Mol. Cell Biol. 13 (2012) 355–369.
[4] N. Yutin, P. Puigbo, E.V. Koonin, Y.I. Wolf, Phylogenomics of prokaryotic ribosomal proteins, PLoS One 7 (2012) e36972.
[5] O. Lecompte, R. Ripp, J.C. Thierry, D. Moras, O. Poch, Comparative analysis of ribosomal proteins in complete genomes: an example of reductive evolution at the domain scale, Nucleic Acids Res. 30 (2002) 5382–5390.
[6] V. Marquez, T. Frohlich, J.P. Armache, D. Sohmen, A. Donhofer, A. Mikolajka, O. Berninghausen, M. Thomm, R. Beckmann, G.J. Arnold, D.N. Wilson, Proteomic characterization of archaeal ribosomes reveals the presence of novel archaeal-specific ribosomal proteins, J. Mol. Biol. 405 (2011) 1215–1232.
[7] J. Wang, I. Dasgupta, G.E. Fox, Many nonuniversal archaeal ribosomal proteins are found in conserved gene clusters, Archaea 2 (2009) 241–251.
[8] K. Brugger, The sulfolobus database, Nucleic Acids Res. 35 (2007) D413–D415.
[9] B.A. Johnson, Using NMRView to visualize and analyze the NMR spectra of macromolecules, Methods Mol. Biol. 278 (2004) 313–352.
[10] J.L. Markley, A. Bax, Y. Arata, C.W. Hilbers, R. Kaptein, B.D. Sykes, P.E. Wright, K. Wuthrich, Recommendations for the presentation of NMR structures of proteins and nucleic acids, J. Mol. Biol. 280 (1998) 933–952.
[11] T. Herrmann, P. Guntert, K. Wuthrich, Protein NMR structure determination with automated NOE assignment using the new software CANDID and the torsion angle dynamics algorithm DYANA, J. Mol. Biol. 319 (2002) 209–227.
[12] A.T. Brunger, P.D. Adams, G.M. Clore, W.L. DeLano, P. Gros, R.W. Grosse-Kunstleve, J.S. Jiang, J. Kuszewski, M. Nilges, N.S. Pannu, R.J. Read, L.M. Rice, T. Simonson, G.L. Warren, Crystallography & NMR system: a new software suite for macromolecular structure determination, Acta Crystallogr. D Biol. Crystallogr. 54 (1998) 905–921.
[13] B.M. Duggan, G.B. Legge, H.J. Dyson, P.E. Wright, SANE (Structure Assisted NOE Evaluation): an automated model-based approach for NOE assignment, J. Biomol. NMR 19 (2001) 321–329.
[14] Y. Shen, F. Delaglio, G. Cornilescu, A. Bax, TALOS+: a hybrid method for predicting protein backbone torsion angles from NMR chemical shifts, J. Biomol. NMR 44 (2009) 213–223.
[15] A.J. Nederveen, J.F. Doreleijers, W. Vranken, Z. Miller, C.A. Spronk, S.B. Nabuurs, P. Guntert, M. Livny, J.L. Markley, M. Nilges, E.L. Ulrich, R. Kaptein, A.M. Bonvin, RECOORD: a recalculated coordinate database of 500+ proteins from the PDB using restraints from the BioMagResBank, Proteins 59 (2005) 662–672.
[16] R. Koradi, M. Billeter, K. Wuthrich, MOLMOL: a program for display and analysis of macromolecular structures, J. Mol. Graph. 14 (1996) 51–55.
[17] R.A. Laskowski, J.A. Rullmannn, M.W. MacArthur, R. Kaptein, J.M. Thornton, AQUA and PROCHECK-NMR: programs for checking the quality of protein structures solved by NMR, J. Biomol. NMR 8 (1996) 477–486.
[18] L. Holm, P. Rosenstrom, Dali server: conservation mapping in 3D, Nucleic Acids Res. 38 (2010) W545–W549.
[19] J.F. Gibrat, T. Madej, S.H. Bryant, Surprising similarities in structure comparison, Curr. Opin. Struct. Biol. 6 (1996) 377–385.
[20] E. Krissinel, K. Henrick, Secondary-structure matching (SSM), a new tool for fast protein structure alignment in three dimensions, Acta Crystallogr. D Biol. Crystallogr. 60 (2004) 2256–2268.
[21] E.F. Pettersen, T.D. Goddard, C.C. Huang, G.S. Couch, D.M. Greenblatt, E.C. Meng, T.E. Ferrin, UCSF Chimera – a visualization system for exploratory research and analysis, J. Comput. Chem. 25 (2004) 1605–1612.
[22] N.A. Farrow, R. Muhandiram, A.U. Singer, S.M. Pascal, C.M. Kay, G. Gish, S.E. Shoelson, T. Pawson, J.D. Forman-Kay, L.E. Kay, Backbone dynamics of a free and a phosphopeptide-complexed Src homology-2 domain studied by ^{15}N NMR relaxation, Biochemistry 33 (1994) 5984–6003.
[23] A.M. Mandel, M. Akke, A.G. Palmer 3rd, Backbone dynamics of *Escherichia coli* ribonuclease HI: correlations with structure and function in an active enzyme, J. Mol. Biol. 246 (1995) 144–163.
[24] R. Cole, J.P. Loria, FAST-Modelfree: a program for rapid automated analysis of solution NMR spin-relaxation data, J. Biomol. NMR 26 (2003) 203–213.
[25] D.L. Mendez, D. Kim, M. Chruszcz, G.E. Stephens, W. Minor, S. Khorasanizadeh, S.C. Elgin, The HP1a disordered C terminus and chromo shadow domain cooperate to select target peptide partners, ChemBioChem 12 (2011) 1084–1096.
[26] T. Wang, C. Xu, Y. Liu, K. Fan, Z. Li, X. Sun, H. Ouyang, X. Zhang, J. Zhang, Y. Li, F. Mackenzie, J. Min, X. Tu, Crystal structure of the human SUV39H1 chromodomain and its recognition of histone H3K9me2/3, PLoS One 7 (2012) e52977.
[27] J.F. Kuhn, E.J. Tran, E.S. Maxwell, Archaeal ribosomal protein L7 is a functional homolog of the eukaryotic 15.5kD/Snu13p snoRNP core protein, Nucleic Acids Res. 30 (2002) 931–941.